

# THE DETAILED RESPONSE FUNCTION INVESTIGATION OF THE FAST NEUTRONS SPECTROMETER BASED ON THE STILBENE CRYSTAL

P.S. Prusachenko, V.A. Khryachkov, V.V. Ketlerov

Institute for Physics and Power Engineering (IPPE), Obninsk, Russia

## 1. Introduction

Organic scintillators are widely used for fast neutron detection [1-3]. However, there are a few problems which give some limitations to used its. One of them relates to low energy region, it is a problem in  $n/\gamma$  separation for low energies. There is a problem for high energy neutrons, it comes from poorly known role of  $(n,\alpha)$  reaction on carbon nuclei, the inelastic scattering on the structural materials of the detector and the influence PMT on response for fast neutrons. All this processes can influence on detector efficiency, and, as a result, on accuracy of neutron spectra measurement. The purpose of our work was to study the influence of the above-mentioned processes on the response of the detector with the stilbene crystal.

## 2. Experimental setup

The measurements were carried out using the time-of-flight method at the Tandetron accelerator in IPPE. The accelerator operated in a pulsed mode. The average pulse width was 1.4 ns. We used  ${}^7\text{Li}(d,n){}^8\text{Be}$  reaction as a fast neutron source. The result of interaction deuteron with infinity thick target was continuous neutron spectrum with a maximum energy up to 22 MeV.

The length of flight path in the experiment was 3 m. The detector was stilbene crystal with size of 40x40 mm. Both signals, and the signal from the detector, and the signal from the accelerator interrupt system were digitized. The waveform digitizer has the sampling rate of 500 MS/s and ADC resolution of 14 bits.

Also, the detector was placed in a specialized neutron shielding. It consists from lead layer with thickness of 10 cm and mixture of paraffin and lithium carbonate with a thickness of 50 cm. The scheme of experimental setup is shown in fig. 1.

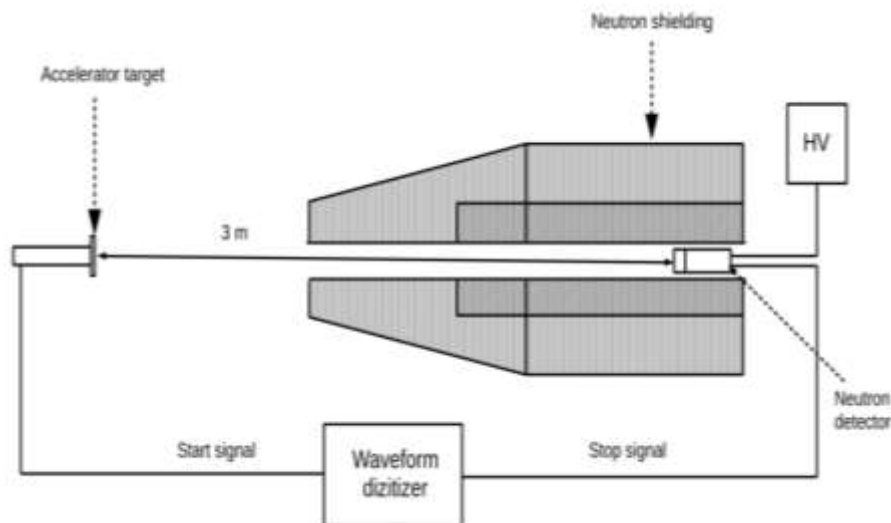


**Fig. 1.** The scheme of experimental setup.

### 3. Signal processing

The correlation analysis was used for digital signal processing. The correlation analysis allows simply and very accurately to determine the start time of the signals, to obtain the signal area and to estimate their shape. The maximum of correlation function is the evaluation of particle type, and its position – the start time of the signal. The methods of signal analysis were described in detail in [1,4]. One of the method's advantages is an opportunity to analyze the signals separated by a small time gap (fig. 2).

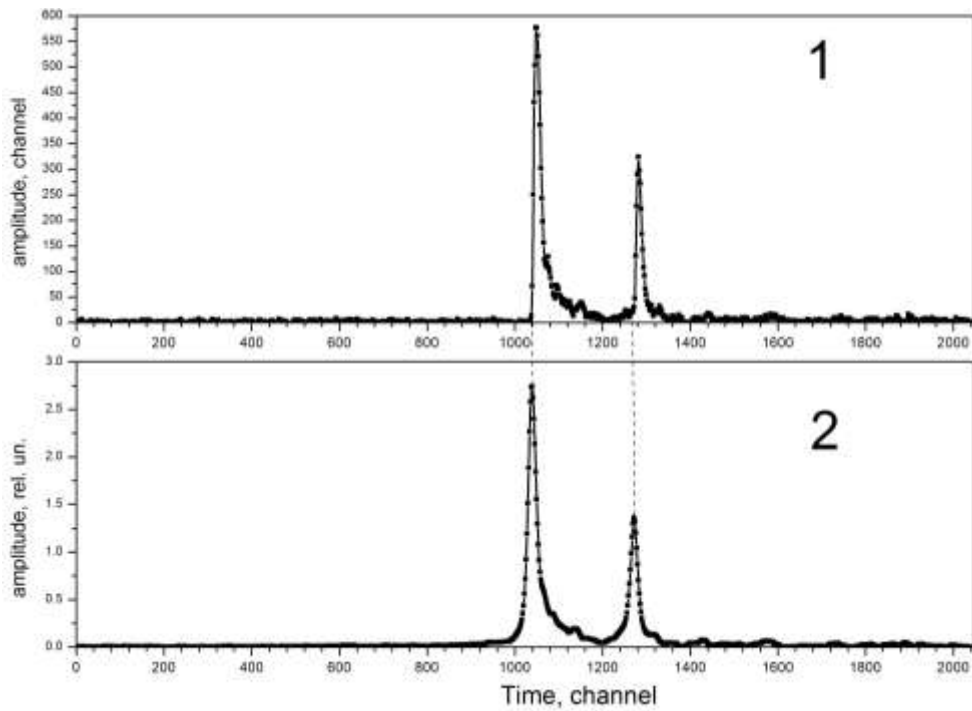


**Fig. 2.** The pile-up signal and correlation function for them.

As the first results of the work, it is possible to demonstrate time-of-flight spectra (fig. 3). In this figure, red points – the array of all signals, blue points – the ToF spectrum after  $n/\gamma$  suppression.

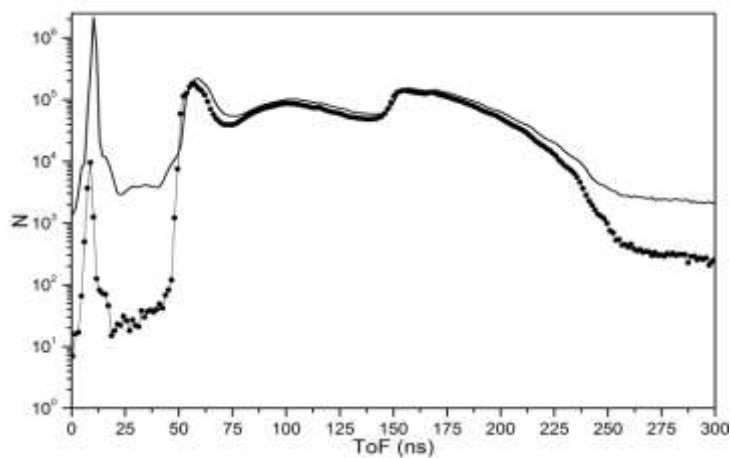


**Fig. 3.** The time-of-flight spectra. Solid line – integral ToF spectrum, points – neutron ToF spectrum after gamma-background suppression.

## 4. Results and discussion

### 4.1. The detector response for the different particle types

The some results of signal processing are shown in fig. 4, a. It is the two-dimensional spectrum, signal's area vs. separation parameter  $R$  obtained from correlation analysis (parameter  $R$ ). We can see three clear separated event's groups and one additional group. We selected the signals from these groups and built the average signal for each of them. This averaged signals are shown in fig. 4, b. We interpreted these groups. Here, there are signals, due to the interaction of gamma rays with the detector material (points in fig. 4, b) and recoil protons (solid line in fig. 4, b). It is also possible to observe a poorly separated from the proton events group of particles, corresponding to alpha-particle from (n, $\alpha$ ) reaction on carbon nuclei (dashed line in fig. 4, b).

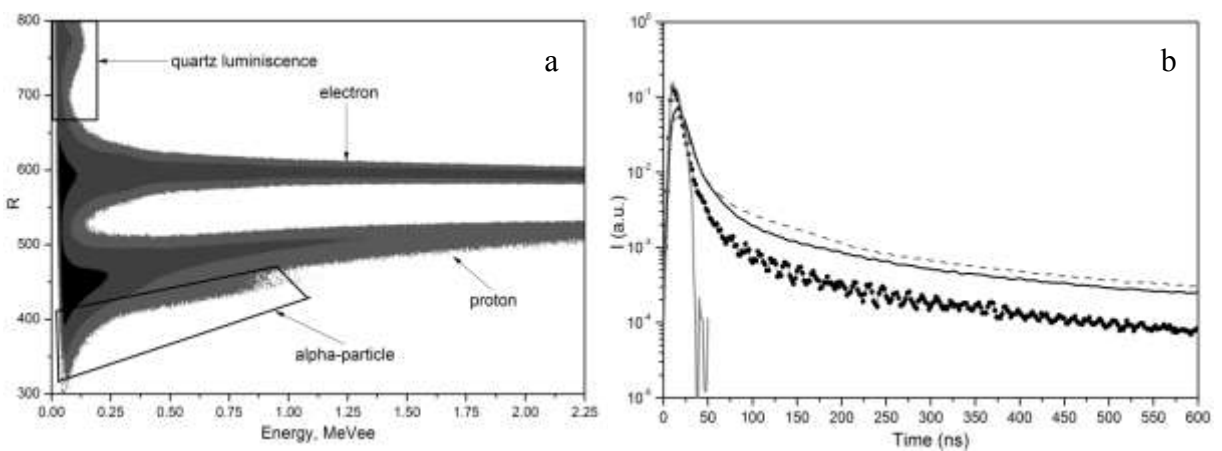


**Fig. 4.** a – signal's area vs. separation parameter; b – response signal for different particle type.

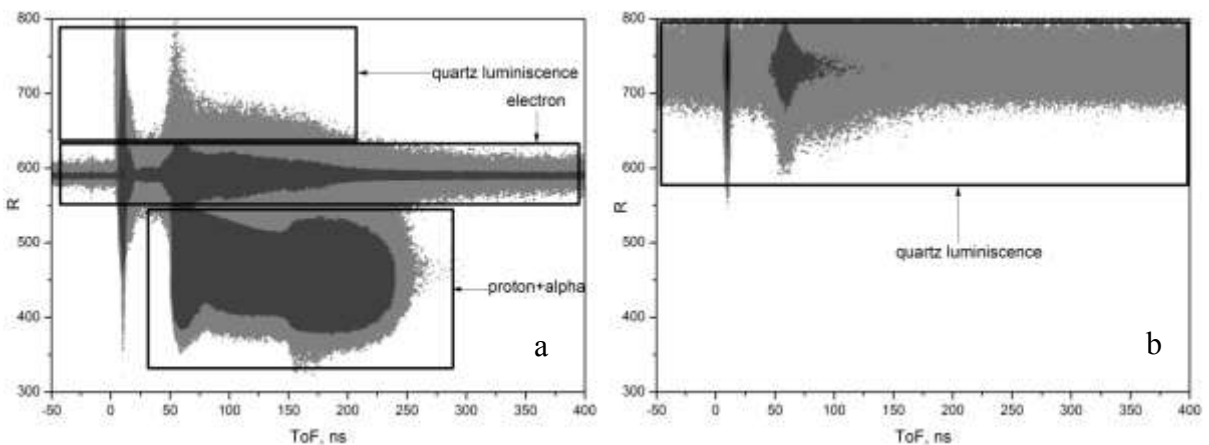


**Fig. 5.** Time-of-flight vs. separation parameter  $R$ . a – experiment with stilbene, b – experiment without stilbene.

The some special case is the group of events that is located above the electrons in fig. 4, a. This events corresponds very short averaged signal without tail (grey line in fig. 4, b). To understand the nature of these signals, the special experiment was done.

In this experiment, we irradiated the detector twice. First time – it was the detector with the

stilbene crystal. Second time – we removed the stilbene crystal from the detector. All other conditions were identical to the first irradiation. The results are shown in fig. 5. In fig. 5 (b), which corresponds with the experiment without stilbene, the events from electron and proton disappeared. But, the group of short events remained on place. We interpreted these events as intrinsic luminescence of quartz input window of PMT. As can be seen from the fig. 4, such events are in the low-energy region. Therefore, for measurements with a low detection threshold, it is important to have a good separation in order to confidently cut off such background events.

#### 4.2. Gamma quanta timing distribution

On the next step of our investigation we tried to understand the shape of gamma-quanta time distribution (fig. 6). In the beginning of the distribution narrow peak corresponding the prompt gamma-ray emission is located. On right side of this peak the many events which appears after the neutron pulse is observed. These events have a clear timing structure. Their timing distribution has a maximum corresponding to small time-of-flight region (the neutrons with high energy). With increasing time-of-flight (and, correspondingly, neutron energy), the number of such gamma quanta decreases. We believe that this gamma-quanta are resulted the inelastic scattering of fast neutron on detector materials. The main element on which the inelastic scattering occurs in the detector is carbon. The inelastic scattering cross-section for carbon contained in stilbene begins to increase sharply after the neutron energy 4.5 MeV. Also in structural materials of the detector is a large number of Al. Inelastic scattering by these two elements will basically determine the time-correlated gamma background for the fast neutron region.

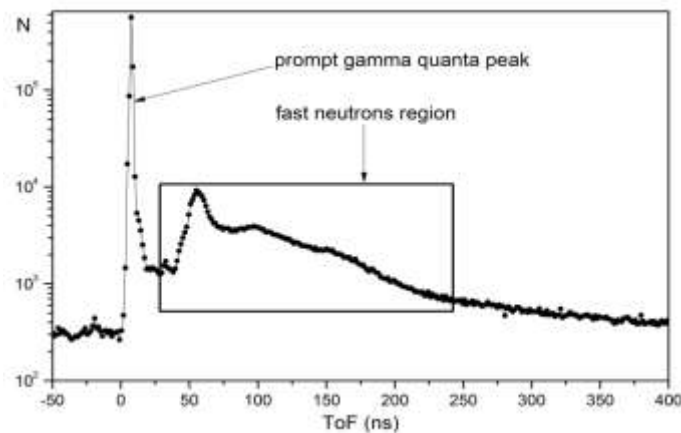


**Fig. 6.** Time-of-flight spectrum for gamma-quanta.

#### 4.3. Light output for alpha-particles and protons

It's well known, that light output in organic scintillators are depended on the ionizing capacity of the particles [5]. The biggest light output corresponds electrons. For protons it is much less. The light output of alpha-particles is poorly studied.

Ionizing capacity for heavy charged particles will be different depending on their energy [3-6]. Therefore, for them, the nonlineardependence of light output on energy will be observed. For electrons, the ionizing capacity is independent of energy. Therefore, the light output for them will depend linearly on the energy of the particles.

Our setup allows to make a direct measurements of light output energy dependence. The two-dimensional spectrum, time-of-flight vs. light output in MeVee, is shown in fig. 7, a. We

selected narrow ranges of time-of-flight separating the neutrons with certain energy. Next, the amplitude distribution for them was built (fig. 7, b). The most right edge of the distribution corresponds the protons obtaining the all energy of incident neutron. Knowing the energy of the incident neutron, we know the energy of the recoil proton and can compare it with the light output of electrons.

The situation for alpha particles is similar to the situation for recoil protons. At the preliminary stage, it is necessary to select events, which according to the separation parameter correspond to alpha particles. The residual nucleus makes practically no contribution to the light output. Therefore, the distribution of amplitudes for reaction products will be due only to alpha particles and will depend on their angular distribution. The right edge of this distribution will correspond to the alpha particles emitted at an angle of 0 degrees. It will have maximum energy. Knowing the neutron energy can easily calculate the energy of the alpha particle emitted at 0 degrees.

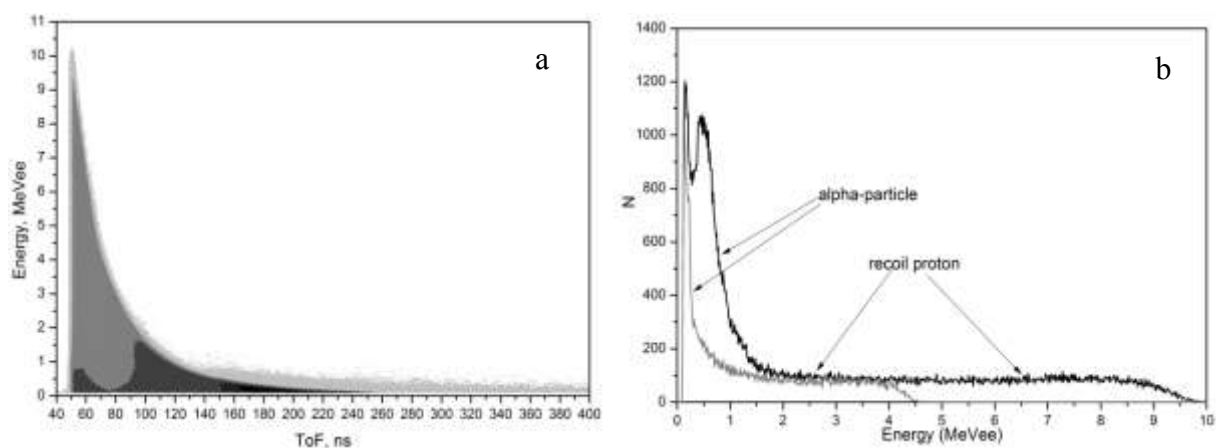


**Fig. 7.** a - time-of-flight vs. light output in MeVee; b - Amplitude distribution of signal for different neutron energy (9 and 18 MeV).

The results are shown in fig. 8. Round points corresponds to recoil protons, square points corresponds to alpha particles. A solid line is the light output for electrons.

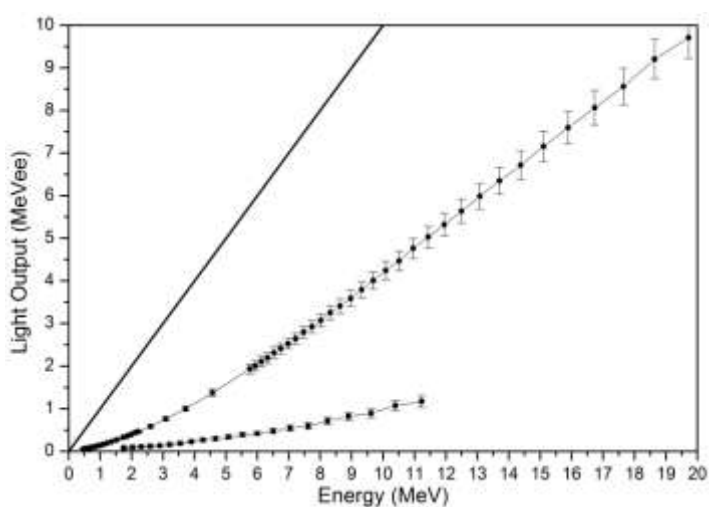


**Fig. 8.** The energy dependence of light output for different particle types. Solid line – electrons, round points – recoil protons, square points – alpha particles.

## 5. Conclusion

Digital spectrometer for fast neutron detection was developed. The response of the spectrometer to the excitation by different particle types was investigated. Influence of quartz window of PMT was studied. It was shown that for low energy region it can be significant. Response signal for this effect was obtained. The role of inelastic scattering of fast neutrons on the carbon nuclei is noted. This leads to a significant increase in the gamma background. The energy dependence of the light output for alpha particles and protons in a wide energy range is obtained. Obtained results allow to better understanding process, which take place during registration process.

## References

- [1] N.V. Kornilov, V.A. Khriatchkov, M. Dunaev, et al., Nuclear Instruments and Methods in Physics Research Section A **497** (2003) 467.
- [2] A. Sardet, C. Varignon, B. Laurent, T. Granier, A. Oberstedt, Nuclear Instruments and Methods in Physics Research Section A **792** (2015) 74.
- [3] N.V. Kornilov, I. Fabry, S. Oberstedt, F.-J. Hamsch, Nuclear Instruments and Methods in Physics Research Section A **599** (2009) 226.
- [4] Prusachenko P.S., Bondarenko I.P., Ketlerov V.V., Khryachkov V.A., Poryvaev V.J., EPG Web of Conferences 146 (2017).
- [5] J. Iwanowska, L. Swiderski, T. Krakowski, Nuclear Instruments and Methods in Physics Research Section A **781** (2015) 44.
- [6] R. A. Cecil, B. D. Anderson, R. Madey, Nuclear Instruments and Methods **161** (1979) 439.